

Lactate Imaging with Hadamard Encoded Slice Selective SelMQC-CSI

S. Pickup¹, S. C. Lee¹, and J. D. Glickson¹

¹Department of Radiology, University of Pennsylvania, Philadelphia, PA, United States

Introduction

Many tumors are known to use glycolytic metabolism instead of oxidative phosphorylation to meet their energy demands even in the presence of an ample supply of oxygen¹. This metabolism combined with compromised tumor perfusion often results in elevated lactate levels. Tumor lactate levels have therefore been proposed as markers for tumor diagnosis², the presence of hypoxia³, therapeutic resistance¹ and poor prognosis⁴. Although tumor lactate concentrations may be determined from biopsy, the metabolism of tumors is known to be heterogeneous and point sampling may not be representative of overall tumor activity. A technique for mapping lactate distributions within the tumor is therefore highly desirable. Magnetic resonance spectroscopy (MRS) has long been recognized as having the potential for providing non-invasive estimates of lactate levels. However, MRS techniques are complicated by the fact that the lactate methyl resonance chemical shift falls in the same range as that for lipids and is thus obscured by the lipid signal unless some spectral editing techniques are applied. The SelMQC technique is a doubly frequency selective, double quantum filtering method that has been shown to be highly selective for lactate⁵. A variation of the SelMQC sequence that includes chemical shift imaging (CSI) gradients has previously been proposed⁵ but was found to lack effective slice selection. Here, a technique that combines the previously described SelMQC-CSI sequence with Hadamard slice selection is described. The utility of the technique in generating slice selective maps of lactate levels is demonstrated in phantoms and subcutaneous tumors.

Methods

All MR studies were performed on a 9.4T vertical bore spectrometer (Varian Inc, Palo Alto, CA) equipped with 55mm 25 G/cm gradients. Axial Hadamard slice selection⁶⁻⁸ and crusher gradients were added to the previously described SelMQC-CSI pulse sequence⁵. Hadamard encoding was achieved using linear combinations of frequency shifted hyperbolic secant pulses. The pulses were designed in pairs having response profiles with inverted symmetry. This method of using $2N$ pulses to generate N th order Hadamard encoding eliminates T_1 contributions to the localization and allows the protocol to be run at reduced TR without degradation of the degree of localization. Multi-band pulses were constructed from single band pulse envelopes by linear combination of frequency shifted single band pulse envelopes.

Phantom studies were performed using a 10 mm high resolution multi-nuclear probe that has been modified for imaging applications (Doty Inc, Columbia, SC). The phantom consisted of a pair of concentric cylinders (5 mm & 10 mm NMR tubes) with a 100 mM lactate solution in the inner volume and mineral oil in the outer volume. To demonstrate slice localization, two oblique planes from the phantom were selected. Animal studies employed a home built 13 mm inner diameter slotted tube resonator developed specifically for the study of xenografts in small animals. SCID mice bearing human non-Hodgkin's lymphoma xenografts were prepared for lactate imaging by induction of general anesthesia with 1% isoflurane in oxygen. Core body temperature was maintained at $35 \pm 3^\circ$ using a fiber optic temperature sensor (inserted rectally) that controlled a warm air source which was directed over the animal. Following generation of T_1 weighted gradient echo scout images, the Hadamard-SelMQC-CSI protocol was run with $TR=2$ sec, $thk = 2$ mm, $FOV = 16 \times 16$ mm², averages = 8, matrix = 16×16 , bandwidth = 4000 Hz and points = 2048 resulting in a total acquisition time of 68 min. All data were processed offline using codes developed in house in the IDL (Research Systems Inc., Boulder, CO) environment for this purpose. The Hadamard transform was applied, followed by two dimensional Fourier transformation. Metabolite maps were then generated by integrating lactate signals in the spectral domain for each pixel.

Results

The gradient echo images of the phantom (Fig-1a,b) clearly depict both volumes within the phantom; lactate and oil. The phantom lactate images (Fig-1c,d) are well correlated with the gradient echo images thus demonstrating the effectiveness of the Hadamard slice localization. The lack of signal from the outer volume of the phantom (Fig-1c,d) demonstrates that the slice selection method did not degrade the lactate specificity.

Fig. 2a,b show gradient echo images of a tumor along with 10 mM lactate phantom (arrowed). Fig. 2c,d show lactate maps obtained from our HD-SelMQC-CSI sequence. Central dark region in a lactate image correlates with the same region in a gradient echo image. The lactate phantom is seen in a lactate image (arrowed) enabling us to estimate that tumor lactate concentration is ~ 10 mM, which is consistent with the level we observed from tumor extract NMR experiments.

Conclusion

Axial Hadamard encoding slice selection has been shown to be an effective method for achieving slice selection in the SelMQC-CSI protocol. Multi-slice lactate maps of the tumor suggest that the HD-SelMQC-CSI technique can reveal lactate distribution inside the tumor slice-selectively *in vivo*.

References

1. Gatenby, R. A.; Gillies, R. J., *Nat Rev Cancer* **2004**, 4, (11), 891-9.
2. Czernicki, Z.; Horsztynski, D.; Jankowski, W.; Grieb, P.; Walecki, J., *Acta Neurochirurgica - Suppl* **2000**, 76, 17-20.
3. Brizel, D. M.; Schroeder, T.; Scher, R. L.; Walenta, S.; Clough, R. W.; Dewhirst, M. W.; Mueller-Klieser, W., *Int J Rad Oncol Biol Phys* **2001**, 51, (2), 349-53.
4. Tedeschi, G.; Lundbom, N.; Raman, R.; Bonavita, S.; Duyn, J. H.; Alger, J. R.; Di Chiro, G., *J Neurosurg* **1997**, 87, (4), 516-24.
5. He, Q.; Shungu, D. C.; van Zijl, P. C.; Bhujwala, Z. M.; Glickson, J. D., *JMR B* **1995**, 106, (3), 203-11.
6. Gonen, O.; Wang, Z. J.; Viswanathan, A. K.; Molloy, P. T.; Zimmerman, R. A., *Amer J Neuroradiol* **1999**, 20, (7), 1333-41.
7. Gonen, O.; Arias-Mendoza, F.; Goelman, G., *MRM* **1997**, 37, (5), 644-50.
8. Dreher, W.; Leibfritz, D., *MRM* **1994**, 31, (6), 596-600.

Fig. 1

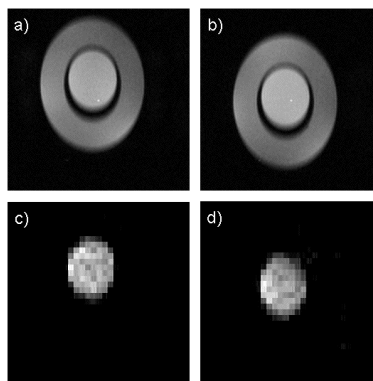


Fig. 2

